

Composition of Primary Cosmic Rays Beyond the “Knee”
from Emulsion Chamber Observations

C. G. S. Costa and F. Halzen

Department of Physics, University of Wisconsin, Madison, WI 53706, USA

J. Bellandi

Instituto de Física Gleb Wataghin, UNICAMP, Campinas, SP 13083-970, Brazil

C. Salles

*Dept. of Materials Science and Engineering,
University of Wisconsin, Madison, WI 53706, USA*

(March 24, 2018)

Abstract

We show that the simplest assumptions for the dynamics of particle production allow us to understand the fluxes of hadrons and photons at mountain altitudes as well as the structure of individual events. The analysis requires a heavy nuclear component of primary cosmic rays above the “knee” in the spectrum with average mass number $\langle A \rangle = 7.3 \pm 0.9$.

PACS number(s): 13.85.Tp, 96.40.De

I. INTRODUCTION

The energy spectrum and chemical composition of primary cosmic rays have been determined from direct observation above the earth's atmosphere using balloons and spacecraft [1]. The technique is limited by the small size of the detectors and the short exposure times. As a result of the steep energy spectrum no direct observations are available above a primary energy of roughly 10^{14} eV. In the interesting region of the “knee” in the spectrum and above information on composition has to be inferred from indirect measurements of air showers at sea level or mountain altitudes [2], by using large area detectors for long periods of time.

In this paper we infer the composition of the cosmic rays from measurements at mountain altitudes of the hadronic and electromagnetic component of the air cascades initiated at the top of the atmosphere. A connection between the nature of the primary particle and air shower observations requires the detailed understanding of particle interactions at very high energies and forward scattering angles where no information is available from accelerator-based experiments. The basic problem is that one is faced with the impossibility of deducing two unknowns, the composition and the dynamics of particle interactions, from a single measurement. We nevertheless pursue this challenge because we are confident that we understand particle interactions with sufficient accuracy to meaningfully approach this problem. We have indeed formulated a model which is based on the most straightforward assumptions and which respects the spirit of quantum chromodynamics [3]. More importantly, it describes in quantitative detail single events, i.e. shower cores in their early stage of development, observed in emulsion chamber experiments at mountain altitudes [4]. Here we will show that this model describes the observed hadronic and electromagnetic spectrum at mountain altitudes, provided the mass number of the primary cosmic rays is $\langle A \rangle = 7.3 \pm 0.9$. This is consistent with the result obtained by other indirect means.

Our model of particle production [3] is guided by the features of QCD-inspired models: approximate Feynman scaling in the fragmentation region and an inelasticity slowly varying

with energy. The rapidity density of secondary charged pions is parametrized as

$$\frac{dN}{dy} = x \frac{dN}{dx} = a \frac{(1-x)^n}{x}, \quad (1)$$

where y is the rapidity of the secondaries and the Feynman variable x is given by the ratio of the energy E of the secondary particle to the incident energy E_0 . With $a = 0.12$ and $n = 2.6$ ($n = 3$ is expected on the basis of counting rules) the overall features of the hadronic component of single events detected in emulsion chambers were quantitatively reproduced. For illustration, we present in Fig. 1 the hadronic integral spectrum of two events detected by the Brazil-Japan Collaboration at Mt. Chacaltaya, Bolivia (atmospheric depth 540 g/cm²) [5,6], which are successfully described by our model [7]. In the present paper we use the same model to calculate both the hadronic and electromagnetic integral spectra of atmospheric showers detected in large emulsion chamber experiments. The calculation is performed by solving the cosmic-ray diffusion equations using the rapidity distribution for particle production given by Eq. (1). Starting with the measured all-particle primary spectrum at the top of the atmosphere, we propagate the particle showers down to the mountain altitude detection levels of the various experiments and investigate our results as a function of the assumed average composition of the primary cosmic radiation.

II. HADRONIC AND ELECTROMAGNETIC SHOWERS IN THE ATMOSPHERE

The flux of cosmic ray nucleons at the top of atmosphere (depth $t = 0$) is parametrized by a power-law spectrum

$$F_n(E, t = 0) = N_0 E^{-(\gamma+1)}. \quad (2)$$

At this point no secondaries have been produced, hence the boundary condition for the pionic component of the shower: $F_\pi(E, t = 0) = 0$. The hadronic flux $F_h(E, t)$ can be calculated for any depth $t = z$ in terms of the interaction mean free path (MFP) of nucleons (n) and pions (π), $\lambda_i(E)$ with $i = n, \pi$. The result is [8]

$$F_h(E, z) = F_n(E, z) + F_\pi(E, z) , \quad (3)$$

with

$$F_n(E, z) = N_0 E^{-(\gamma+1)} e^{-zH_n(E)} , \quad (4)$$

$$F_\pi(E, z) = N_0 E^{-(\gamma+1)} \frac{g_n(\gamma, E)}{H_n(E) - H_\pi(E)} \times \left(e^{-zH_\pi(E)} - e^{-zH_n(E)} \right) . \quad (5)$$

The dependence of the functions $H_i(E)$ and $g_i(\gamma, E)$ on the rapidity distribution, Eq. (1), and on the MFP $\lambda_i(E)$, is described in the Appendix.

The electromagnetic component of the shower is initiated by gamma rays from the decay of the neutral pion, $\pi^0 \rightarrow 2\gamma$. With equal multiplicity of π^+ , π^- and π^0 secondaries, the number of neutral pions is half the number of the charged pions which is given by Eq. (5). The gamma-ray distribution is given by two-body decay [9]

$$\mathcal{F}_\gamma(E_\gamma, z) dE_\gamma dz = 2 \int_{E_\gamma}^{\infty} \frac{dE}{E} \frac{1}{2} F_\pi(E, z) dE_\gamma dz . \quad (6)$$

A gamma ray with energy E_γ at depth z contributes to the electromagnetic cascade $F_\gamma(E, t)$ with

$$F_\gamma(E, t) = \int_0^t dz \int_{E_\gamma}^{\infty} dE_\gamma \mathcal{F}_\gamma(E_\gamma, z) \times (e + \gamma)(E_\gamma, E, t - z) . \quad (7)$$

Here $(e + \gamma)(E_\gamma, E, t - z)$ represents the photons and e^+e^- pairs in the cascade produced by the photon with energy E_γ . We compute it in approximation A [10] using the operator formalism [11]. The result is of the form of Eq. (7) with $(e + \gamma)(E_\gamma, E, t - z)$ given by the eigenvalues of the electromagnetic cascade equations; see Appendix.

We are now ready to compute the integral energy spectrum for hadrons and photons ($i = h, \gamma$),

$$I_i(> E, z) = \int_E^{\infty} F_i(E', z) dE' , \quad (8)$$

which can be confronted with experimental results.

III. INELASTIC CROSS SECTION FOR HADRON-AIR INTERACTIONS

Before proceeding with the analysis, it is necessary to describe the energy dependence of the MFP which is inversely proportional to the inelastic cross section for hadron-air interactions, i.e.

$$\lambda_i(E) = \frac{24,100(\text{g/cm}^2)}{\sigma_{\text{in}}^{\text{i-air}}(\text{in mb})} . \quad (9)$$

We calculated the inelastic cross section using the event generator SIBYLL [12]. The result can be parametrized by

$$\sigma_{\text{in}}^{\text{i-air}} = s_i \left[1 + b_i \ln^2 \left(\frac{E}{E_0} \right) \right] , \quad (10)$$

with $E_0 = 200$ GeV. Our results with $s_n = 284.5$ mb and $b_n = 3.852 \times 10^{-3}$ for proton-air and $s_\pi = 211.0$ mb and $b_\pi = 5.827 \times 10^{-3}$ for pion-air scattering are shown in Fig. 2.

IV. PRIMARY COMPOSITION AND SHOWER ENERGY SPECTRA

Having constructed an explicit model of particle interactions which successfully describes individual events, see Fig. 1, we can compute the flux of hadrons and photons at mountain altitude as a function of the primary cosmic ray flux. For the primary spectrum we use a parametrization [13] which is accurate in the energy region between 300 and 10^6 TeV/particle relevant to our calculation. It accurately extrapolates to lower energy measurements obtained with the Proton satellite and the JACEE balloon flights [13,14]. The all-particle differential energy spectrum, is given by

$$F_{\text{all}}(E, t = 0) = (4.55 \pm 0.45) \times 10^{-11} \left[\frac{E}{10^{3.67}} \right]^{-(\gamma+1)} , \quad (11)$$

in units of $(\text{m}^2 \text{ sec sr TeV/particle})^{-1}$, with $\gamma = 1.62 \pm 0.12$ below and $\gamma = 2.02 \pm 0.05$ above $10^{3.67}$ TeV/particle. Eq. (11) describes the change in the slope of the spectrum at the energy region known as “the knee”. We parametrize our ignorance of the chemical composition of the primary flux in terms of a single parameter $\langle A \rangle$, the average mass number of the

primary nuclei. Heavy primaries are included in our formalism using superposition [2] in Eq. (2). The projectile nucleus of energy E_0 is considered to be the superposition of A nucleons interacting independently, each having energy E_0/A . Although a simplification, this assumption is quite acceptable, as long as the nuclei fragment relatively rapidly.

We first calculate the integral energy spectra of electromagnetic showers, Eq. (8), at the detection level of Mt. Chacaltaya, using the extremes values for $\langle A \rangle$ corresponding to pure proton ($A = 1$) and to pure iron ($A = 56$). The results are shown in Fig. 3, by the dashed curves. The predictions bracket the experimental data [15]. That a pure proton spectrum cannot describe these results is not totally surprising [16]. It is well known that the relatively low rate of detected gamma-ray families (and also of halo families) cannot be understood in models with approximate Feynman scaling unless heavy primaries contribute to the cosmic ray flux. We subsequently determine, by chi-square minimization, the average mass number that best describes the data. We obtain $\langle A \rangle = 7.3 \pm 0.9$ (solid line in Fig. 3).

Having fixed all parameters, we can confront the model with any other observations. We find that it successfully describes both the hadronic (Fig. 4a) and electromagnetic (Fig. 4b) components of the atmospheric showers detected in large emulsion chambers at Mt. Fuji [17] in Japan (atmospheric depth 650 g/cm^2), and at Mt. Kanbala [18] in China (520 g/cm^2).

V. CONCLUSIONS

We conclude that with the simplest assumptions for the production of secondaries based on approximate scaling in the fragmentation region, it is possible to explain a broad set of experimental data on very high energy cosmic rays in the atmosphere, namely the lateral spread and the integral spectra of superfamilies (as in Ref. [3] and Fig. 1), and the energy spectra of hadronic and electromagnetic showers detected in large emulsion chamber experiments (as in Figs. 3 and 4). This scenario requires a primary composition with average mass number 7.3 ± 0.9 . We investigated the sensitivity of this quantity to different parametrizations of the all-particle spectrum [19,20] and the best fit invariably yields $\langle A \rangle \simeq 7$. Our

result is also consistent with underground muon measurements [21] which yield an A -value of 10 ± 4 in the 1 to 1,000 TeV energy range.

It has been noted elsewhere [22] that it is difficult to establish whether one must adopt a heavy primary composition along with a model of particle production based on scaling or, alternatively, a proton dominant composition along with a strong violation of Feynman scaling. It should be noted however that in our analysis the particle interaction model was determined on the basis of an independent study of single events initiated by protons deep in the atmosphere. The a posteriori analysis of the hadron and photon spectra at mountain altitude presented here, required the introduction of heavy primaries.

ACKNOWLEDGMENTS

This research was supported in part by the Conselho Nacional de Desenvolvimento Científico e Tecnológico (CNPq, Brazil), in part by the U.S. Department of Energy under Grant No. DE-FG02-95ER40896, and by the National Science Foundation under Contract No. DMR-9319421, and in part by the University of Wisconsin Research Committee with funds granted by the Wisconsin Alumni Research Foundation.

APPENDIX: DEFINITIONS IN THE ANALYTICAL SOLUTIONS

Complete definition of the hadronic flux components presented in Eqs. (4) and (5) requires the following functions (for $i = n, \pi$):

$$H_n(E) = \frac{1}{\lambda_n(E)} \left(1 - \frac{1}{2} \langle \sigma_n^\gamma \rangle \right) - \frac{1}{2} \left\langle \frac{\sigma_n^\gamma}{\lambda_n(E/\sigma_n)} \right\rangle, \quad (\text{A1})$$

$$H_\pi(E) = \frac{1}{\lambda_\pi(E)} \left(1 + \frac{1}{2} \langle \sigma_\pi^\gamma \rangle + \frac{1}{2} g_\pi(\gamma) \right) - \frac{3}{2} \left\langle \frac{\sigma_\pi^\gamma}{\lambda_\pi(E/\sigma_\pi)} \right\rangle - g_n(\gamma, E), \quad (\text{A2})$$

$$g_i(\gamma, E) = \int_0^1 \frac{1}{\lambda_i(E/x)} \frac{dN}{dx} x^\gamma dx, \quad (\text{A3})$$

with

$$\begin{aligned}
g_i(\gamma) &= \int_0^1 \frac{dN}{dx} x^\gamma dx , \\
\langle \sigma_i^\gamma \rangle &= \int_0^1 f(\sigma_i) \sigma_i^\gamma d\sigma_i , \\
\left\langle \frac{\sigma_i^\gamma}{\lambda_i(E/\sigma_i)} \right\rangle &= \int_0^1 \frac{1}{\lambda_i(E/\sigma_i)} f(\sigma_i) \sigma_i^\gamma d\sigma_i .
\end{aligned}$$

The elasticity distribution is assumed to be

$$f(\sigma_i) = (1 + \beta) (1 - \sigma_i)^\beta , \quad (\text{A4})$$

where β fulfills a consistency relation between average elasticity $\langle \sigma \rangle$ and average inelasticity $\langle K \rangle$, so that $\langle \sigma \rangle + \langle K \rangle = 1$ (energy conservation). The eigenvalues for the electromagnetic cascade equations are [11]

$$\begin{aligned}
\Pi_\gamma(s, t) &= \frac{1}{X_0} \frac{B(s)}{(\lambda_1(s) - \lambda_2(s))} \\
&\quad \times \left(e^{\lambda_1(s)t/X_0} - e^{\lambda_2(s)t/X_0} \right) , \quad (\text{A5})
\end{aligned}$$

$$\begin{aligned}
\Gamma_\gamma(s, t) &= \frac{1}{X_0} \left(H_2(s) e^{\lambda_1(s)t/X_0} \right. \\
&\quad \left. + H_1(s) e^{\lambda_2(s)t/X_0} \right) , \quad (\text{A6})
\end{aligned}$$

where $H_1(s), H_2(s), \lambda_1(s), \lambda_2(s)$ and X_0 are parameters with standardized definitions in cascade theory [10]. Subsequently $(e + \gamma)(E_\gamma, E, t - z)$ in Eq. (7) should be replaced by $(\Pi_\gamma(s, t - z) + \Gamma_\gamma(s, t - z))$ with s evaluated at the pole $s = \gamma$.

REFERENCES

- [1] For a recent review, see T. Shibata, in *Rapporteur Talk presented at the 24th International Cosmic Ray Conference* (Rome, Italy, 1995), University of Tokyo ICRR-Report-343-95-9, 1995.
- [2] T.K. Gaisser, in *Cosmic Rays and Particle Physics*, (Cambridge University Press, Cambridge, 1992).
- [3] C.G.S. Costa, F. Halzen and C. Salles, *Phys. Rev. D* **52**, 3890 (1995).
- [4] C.M.G. Lattes, Y. Fujimoto and S. Hasegawa, *Phys. Rep.* **65**, 151 (1980).
- [5] J.A. Chinellato, Ph.D Thesis, Universidade Estadual de Campinas, Brazil (1981).
- [6] Brazil-Japan Collaboration, J.A. Chinellato *et al.*, in *Proc. of the 21st International Cosmic Ray Conference*, Adelaide, Australia, ed. by R.J. Protheroe (Graphic Services, Northfield, 1990), Vol. 8, p. 259.
- [7] The drawback of using analytic shower theory is the neglect of fluctuations. This is not a problem here as their effect is masked by the fact that average depth and energy of the incident particle are fitted as parameters. These should have acceptable values [3], but cannot be rigorously interpreted on an event by event basis. The procedure is equivalent to averaging several events.
- [8] J. Bellandi *et al.*, *Nuovo Cimento C* **14**, 15 (1991).
- [9] C.E. Navia *et al.*, *Phys. Rev. D* **40**, 2898 (1989).
- [10] J. Nishimura, in *Handbuch der Physik*, ed. by K. Sitte (Springer, Berlin, 1967), Vol. 62, Part 2, p. 1 .
- [11] J. Bellandi Fo. *et al.*, *J. Phys. A: Math. Gen.* **25**, 877 (1992).
- [12] R.S. Fletcher, T.K. Gaisser, P. Lipari and T. Stanev, *Phys. Rev. D* **50**, 5710 (1994).
- [13] T. Hara *et al.*, in *Proc. of the 18th International Cosmic Ray Conference*, Bangalore, India, 1983, ed. by N. Durgaprasad *et al.* (CTIFR, Bombay, 1983), Vol. 9, p. 198; see

- also, M. Nagano *et al.*, *J. Phys. G* **10**, 1295 (1984).
- [14] JACEE Collaboration, K. Asakimori *et al.*, in *Proc. of the 7th International Symposium on Very High Energy Cosmic Ray Interactions*, Tokyo, Japan, ed. by Y. Fujimoto *et al.*, (Tokyo, 1994), p. 513.
- [15] Brazil-Japan Collaboration, C.M.G. Lattes *et al.*, *Prog. Theor. Phys. Suppl.* **47**, 1 (1971); and in *Proc. of the 13th International Cosmic Ray Conference*, Denver, USA, (Colorado Associated Univ. Press, Boulder, 1973), Vol. 3, p. 2219.
- [16] M. Shibata, *Phys. Rev. D* **24**, 1847 (1981); J.R. Ren *et al.*, *Phys. Rev. D* **38**, 1404 (1988).
- [17] Mt. Fuji Collaboration, M. Akashi *et al.*, *Nuovo Cimento A* **65**, 355 (1981).
- [18] China-Japan Emulsion Chamber Collaboration, J.R. Ren *et al.*, *Nuovo Cimento C* **10**, 43 (1987).
- [19] JACEE Collaboration, T.H. Burnett *et al.*, in *Proc. of the International Symposium on Cosmic Ray and Particle Physics*, Tokyo, Japan, ed. by A. Ohsawa and T. Yuda (Yamada, Tokyo, 1984), p. 468.
- [20] B. Wiebel-Sooth, P.L. Biermann and H. Meyer, in *Proc. of the 24th International Cosmic Ray Conference*, Rome, Italy (INFN, Rome, 1995), Vol. 2, p. 656.
- [21] MACRO Collaboration, in *Proc. of the 24th International Cosmic Ray Conference*, Rome, Italy (INFN, Rome, 1995), Vol. 2, p. 689.
- [22] T. Yuda, in *Rapporteur Talk presented at the 22nd International Cosmic Ray Conference*, (Dublin, Ireland, 1991), Vol. 5, p. 313; F. Halzen, in *Proc. of VII International Symposium on Very High Eenergy Cosmic Ray Interactions*, Ann Arbor, USA, ed. by L. Jones (AIP, New York, 1993), AIP Conf. Proc. Vol. 276, p. 679.

FIGURES

FIG. 1. Integral energy spectra of hadronic superfamily events detected at Mt. Chacaltaya [5,6]. Ursa Maior event (\diamond) and Centauro VII data (\triangle), are compared to the calculation of Ref. [3] (solid line), using the x -distribution of Eq. (1). For illustrative purposes, the data of Centauro VII have been shifted by a factor 10.

FIG. 2. Inelastic cross sections for p -air (\circ) and π -air (\square) scattering computed using SIBYLL [12] and parameterized by Eq. (10).

FIG. 3. Integral energy spectra of electromagnetic showers (\diamond), detected at Mt. Chacaltaya [15], compared to the calculation using the x -distribution of Eq. (1). Dashed lines: $\langle A \rangle = 1$ (proton) and 56 (iron); solid line: $\langle A \rangle = 7.3 \pm 0.9$, dotted lines: calculated from uncertainties in A and γ .

FIG. 4. Integral energy spectra of showers detected at Mt. Fuji [17] (\circ) and Mt. Kanbala [18] (\triangle), compared to the analytical calculation using the x -distribution of Eq. (1), with $\langle A \rangle = 7.3 \pm 0.9$ (solid line). (a) Hadron induced showers; (b) Electromagnetic showers. The data of Mt. Kanbala have been shifted by a factor 100. Dotted lines are calculated from uncertainties in A and γ .

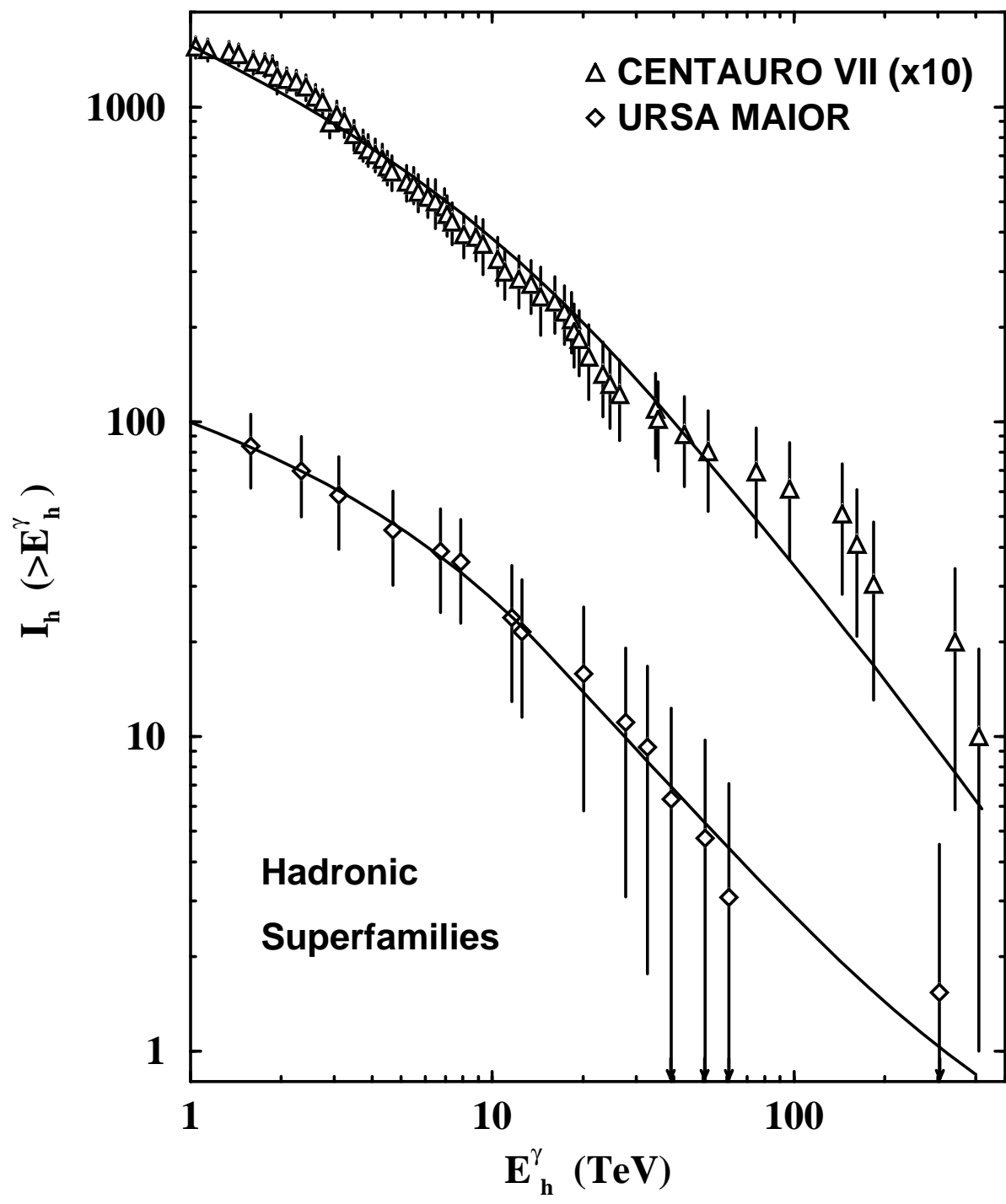


Fig. 1

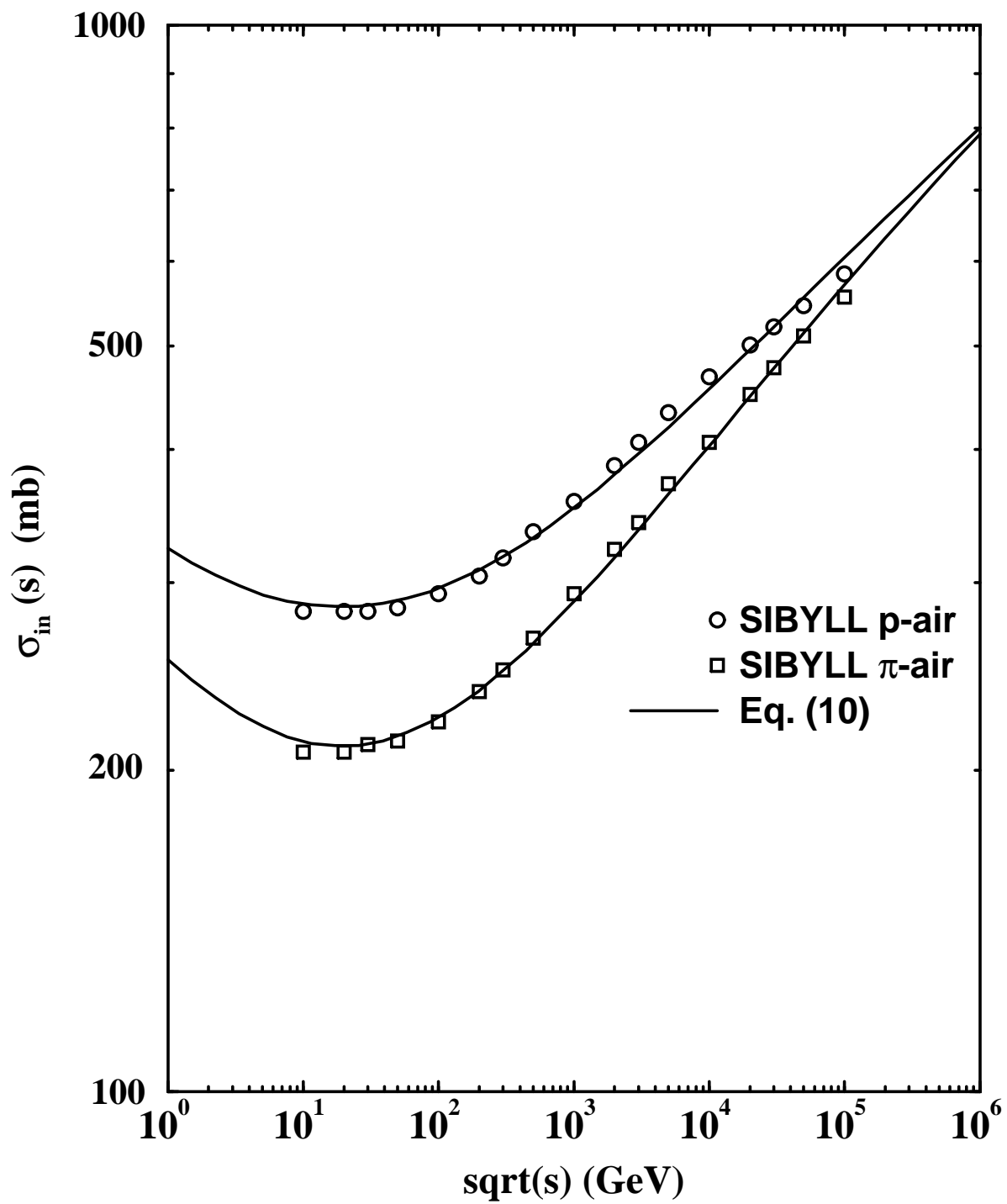


Fig. 2

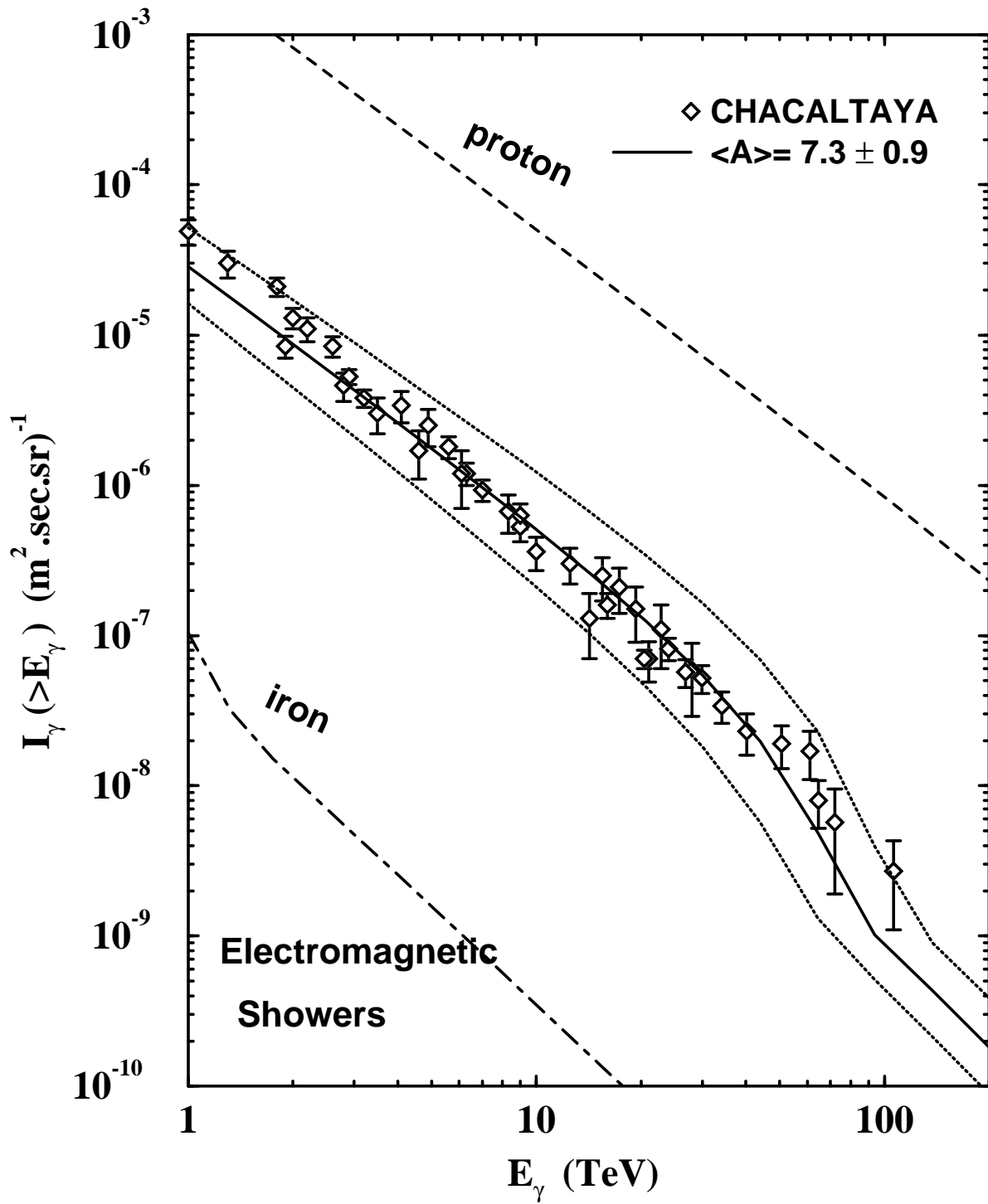


Fig. 3

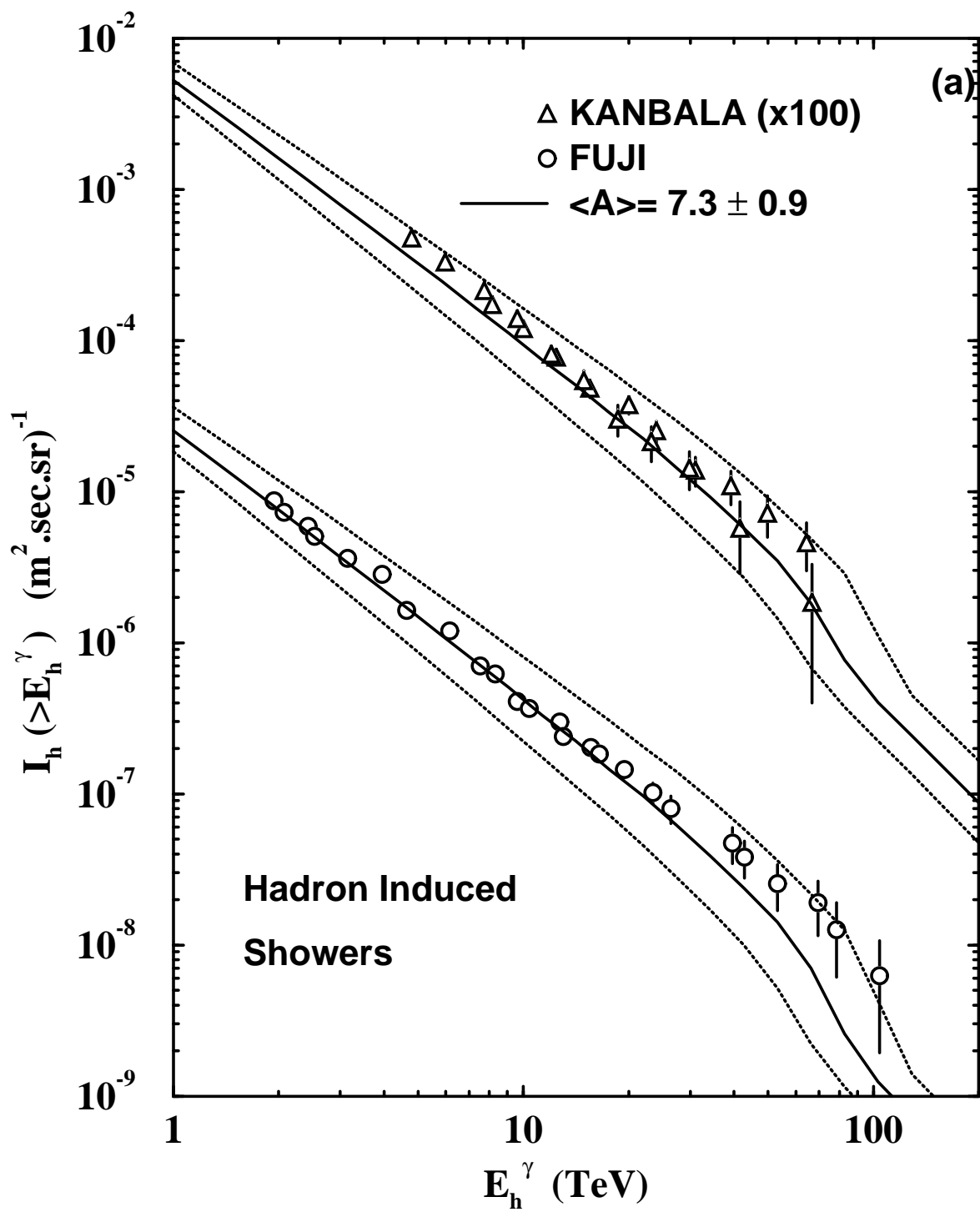


Fig. 4a

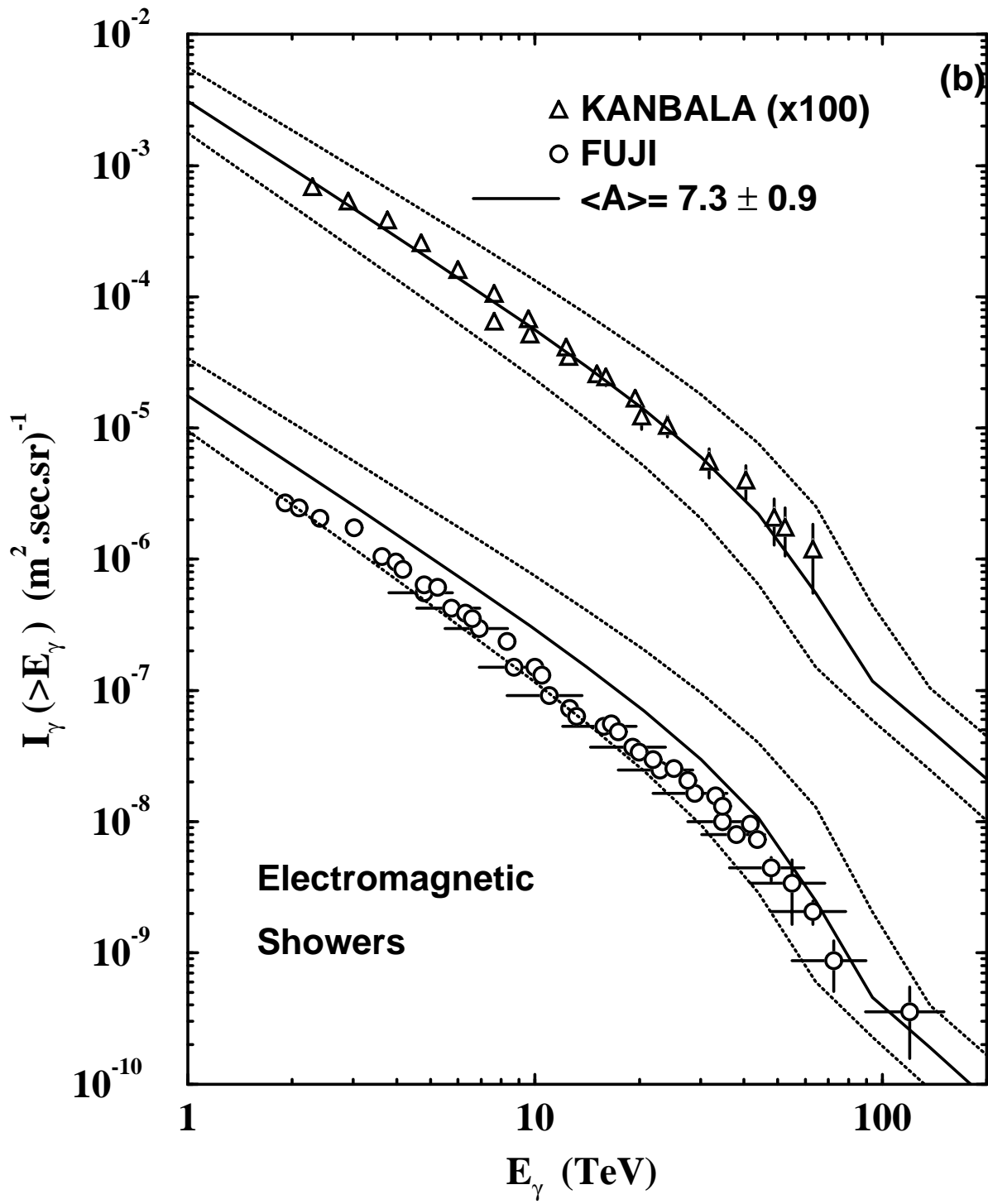


Fig. 4b